Title
NEGATIVE MASS INSTABILITIES IN AN ELECTRON-RING COMPRESSOR

Authors
Entis, A.C.
Garren, A.
Smith, L.

Publication Date
1971-02-01

Presented at the Particle
Accelerator Conference,
Chicago, Ill., March 1-3, 1971

UCRL-20208
Preprint

NEGATIVE MASS INSTABILITIES IN AN ELECTRON-RING COMPRESSOR

A. C. Entis, A. A. Garren, and L. Smith

February 1971

AEC Contract No. W-7405-eng-48

LAWRENCE RADIATION LABORATORY
UNIVERSITY of CALIFORNIA BERKELEY

UCRL-20208

DISCLAIMER

NEGATIVE MASS INSTABILITIES IN AN ELECTRON-RING COMPRESSOR*

A.C. Entis, A.A. Garren, and L. Smith

Lawrence Radiation Laboratory
University of California
Berkeley, California

Introduction

Experiments on Compressor 4 at LRL[1] show strong evidence of a negative mass instability which develops immediately after injection and generates such a large energy spread that the achievement of electron densities in a range of interest for trapping and accelerating ions becomes very difficult. A theoretical analysis of this phenomenon consists of applying the usual dispersion relations to determine a recommended energy spread in the injected beam sufficient to prevent modulations in beam intensity from growing. The essential ingredient in such an analysis is the relation of the electric field component in the direction of motion to the modulation amplitude. Unfortunately, this relation is very sensitive to the immediate environment which, in reality, consists of a ceramic vacuum chamber, possibly coated with metal, and various metallic structures necessary for proper injection of the electron beam.

Such a configuration cannot be easily represented by a tractable mathematical model. We have chosen to explore the consequences of two relatively simple models for the compressor; first, a straight ceramic tube coated with a thin metallic layer and second, a metallic pillbox with lossy walls. The first model accounts for the significant materials seen by the beam, whereas the second model provides a more realistic representation of the compressor geometry. In the range of coating thicknesses experimentally available, bounded on the low side (~ 100 ohms/square) by the difficulty of maintaining a uniform coating in the presence of the beam and on the high side (~ 5 ohms/square) by the requirement that the inflecting field should penetrate the wall, the two models lead to much the same results, and are in rough agreement with experimental observations.

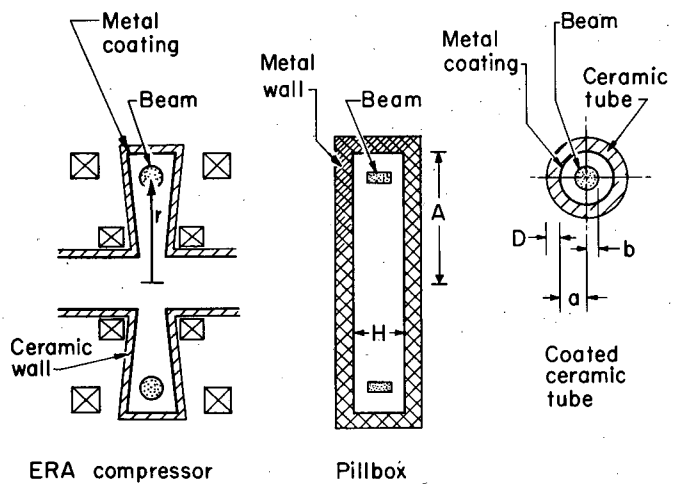

Fig. 1. Schematic diagrams of the LRL ERA Compressor and of the pillbox and straight ceramic tube models.

Both models predict a resonant enhancement of the azimuthal electric field at frequencies in the range through which the beam must pass during compression.

* Work supported by the U.S. Atomic Energy Commission.

In principle, the dispersion equation should be handled with special care in a resonant situation, but since we shall be most interested in Q-values of the order of 10 or less, we have contented ourselves with a simpler and more conservative criterion for the required energy spread. Furthermore, these coatings are thin compared to skin depth at the frequencies of interest (~ 10^9 Hz), so that the surface resistance, R_s, measured in ohms/square is the parameter of interest with respect to the coating.

Schematic diagrams of the compressor and the two idealizations are shown in Fig. 1.

Ceramic Tube Model

Consider a straight, infinitely long, tube of dielectric material of arbitrary inner and outer radius, coated on the inner radius with a metallic layer of arbitrary conductivity and thickness. Down the axis of this tube flows a beam of electrons, uniform in cross-section but with a density modulation proportional to $e^{i(kz-\omega t)}$ (see Fig. 1). The longitudinal electric field in the vicinity of the beam has been calculated with a computer program developed, and generously supplied to us, by Dr. B. Zotter of CERN[2]. This program solves Maxwell's equations for the given beam modulation by matching suitable combinations of Bessel functions at the various interfaces.

The wave number k and linear displacement z for the pipe correspond to n/r and $r\theta$ for a circular beam, where r is the major radius of the beam and n is the harmonic number of the density modulation. The perturbed charge density per unit length, defined as

$$\frac{eN_n}{2\pi r} e^{i(n\theta-\omega t)} , \qquad (1)$$

gives rise to an azimuthal electric field averaged over the beam cross-section of the form $\langle E_n \rangle e^{i(n\theta-\omega t)}$. It is convenient to introduce the dimensionless complex number g_n defined by[3]

$$\langle E_n \rangle = -\frac{ienN_n}{2\pi r^2\gamma^2} g_n , \qquad (2)$$

where $\gamma = (1 - \beta^2)^{-\frac{1}{2}}$, $\beta = v/c$.

The parameter g_n for the pipe is presented in Figs. 2 through 5. In Fig. 2a, g_n is presented for an injection energy of 2.3 MeV at an injection radius of 18 cm, (injection conditions in the current compressor experiments) as a function of mode number n and surface resistance R_s. The beam has a minor radius of 1.5 cm and the pipe has an inside radius $a = 4.1$ cm, a wall thickness $D = 1.6$ cm and a dielectric constant $\epsilon = 8$. Figure 2b shows the same calculation for an injection energy of 4.0 MeV, an energy that will be accessible following injector modifications.

The graphs show the two lowest dielectric resonances at mode numbers 7 and 19. The resonant mode numbers are given approximately by[2]

$$n = \frac{\pi}{\sqrt{\epsilon - 1}} \frac{r}{D} (3/4 + m), \quad m = 0,1,2 \cdots, \qquad (3)$$

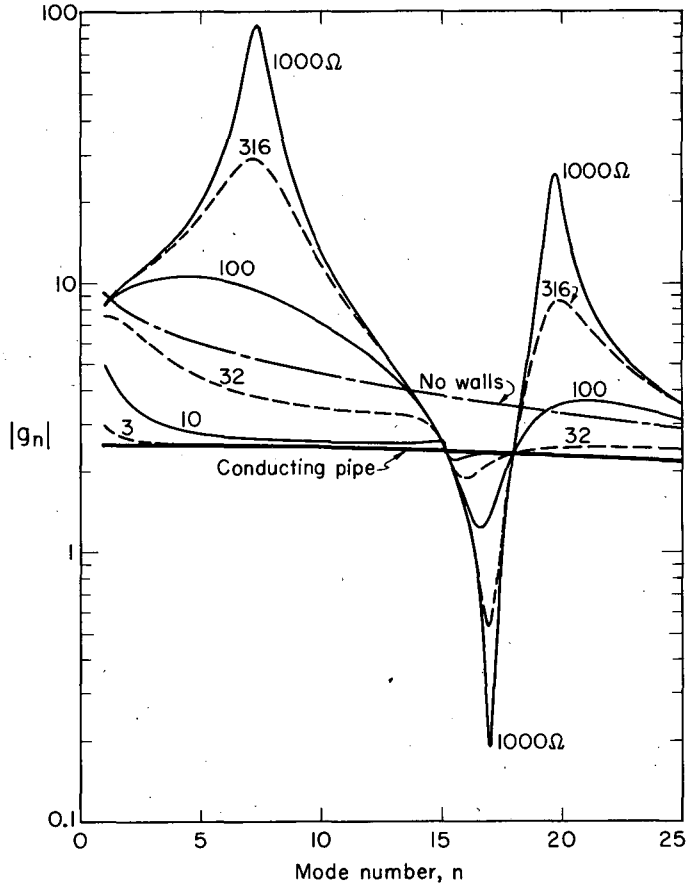

Fig. 2a. Ceramic tube model. Longitudinal field coefficient $|g_n|$ vs mode number n for different R_s values, with r = 18 cm, b = 1.5 cm, a = 4.1 cm, D = 1.6 cm, and T = 2.3 MeV.

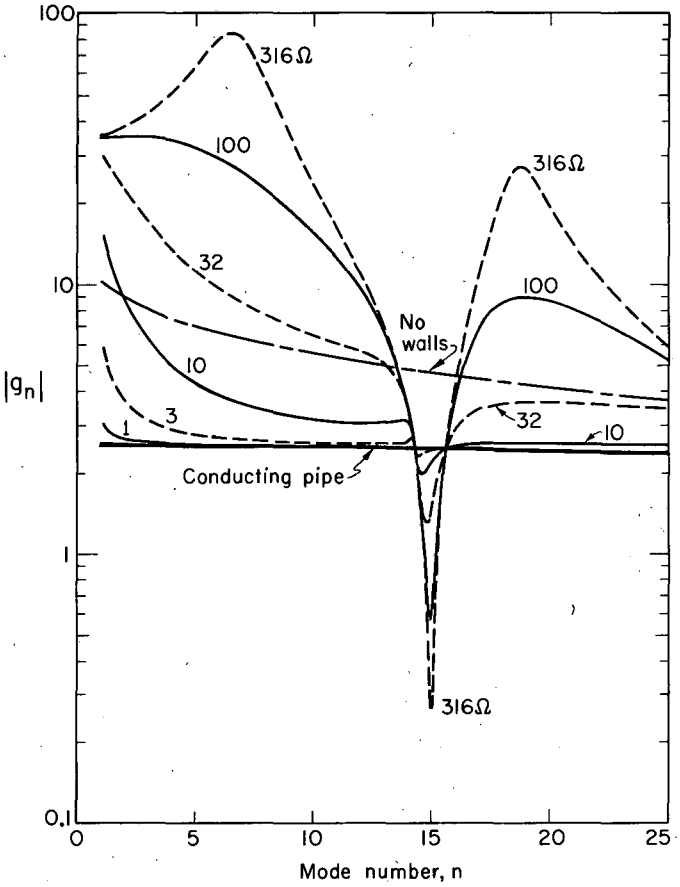

Fig. 2b. Ceramic tube. $|g_n|$ vs n for T = 4.0 MeV.

Their strengths decrease rapidly with n. For values of the surface resistance of the order of 50Ω, the resonant behavior disappears, and the g_n values approximate those for a beam in empty space, $g_n = [\frac{1}{2} - 2\ell n\,(\frac{n}{r}\frac{b}{\gamma})]$.[2] As R_s is further decreased to a few ohms/square, g_n approaches the value for a beam in a conducting pipe, $g_n = \frac{1}{2} + 2\ell n(a/b)$, which is equal to 2.5 for a = 4.1 cm and b = 1.5 cm.

Figure 3 shows $|g_n|$ for the first ten modes as a function of orbit radius during a compression cycle, for injection energy 2.3 MeV and R_s = 1000 ohms/square. Beam momentum and minor radius are scaled as 1/r and r respectively during compression. The pipe radius has also been scaled to correspond to the wall separation of the compressor as r decreases. Peaks occur in $|g_n|$ when the wavelength of the perturbing charge density is resonant with the pipe. This happens for radii and mode numbers such that $\lambda = \frac{2\pi r}{n}$ where λ is a resonant wavelength. The peaks in Fig. 3 correspond to m = 0 in equation (3).

Only the upper envelope of the curves in Fig. 3 is important for stability. The envelope is graphed against r in Fig. 4 for different resistances R_s. Figure 5 shows the influence of wall radius and resistance on $|g_n|$. For large values of R_s the walls should be far from the beam and for $R_s \leq 1\Omega$ the walls

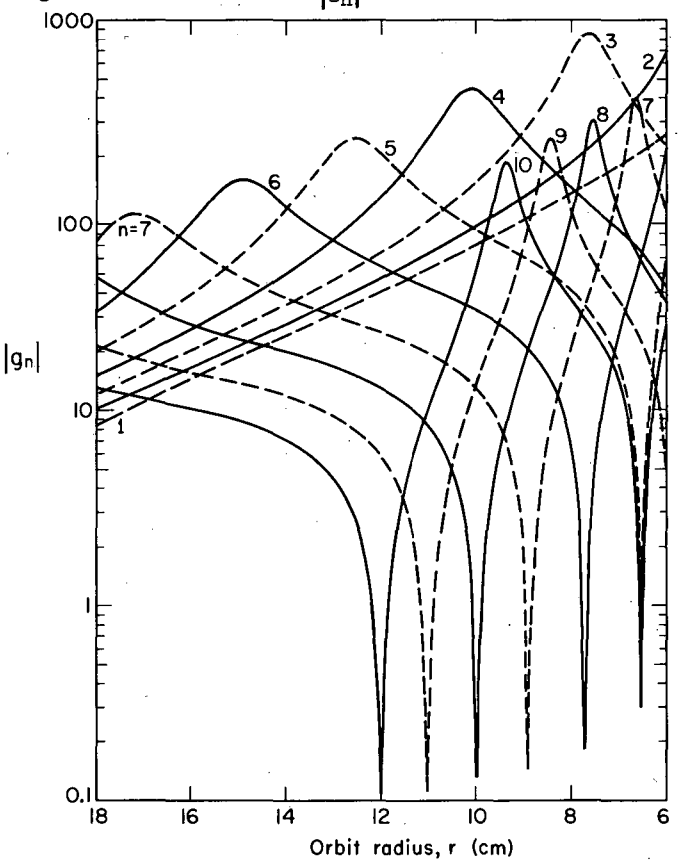

Fig. 3. Ceramic tube. $|g_n|$ (n = 1-10) vs orbit radius r of a ring during compression, R_s = 1000Ω.

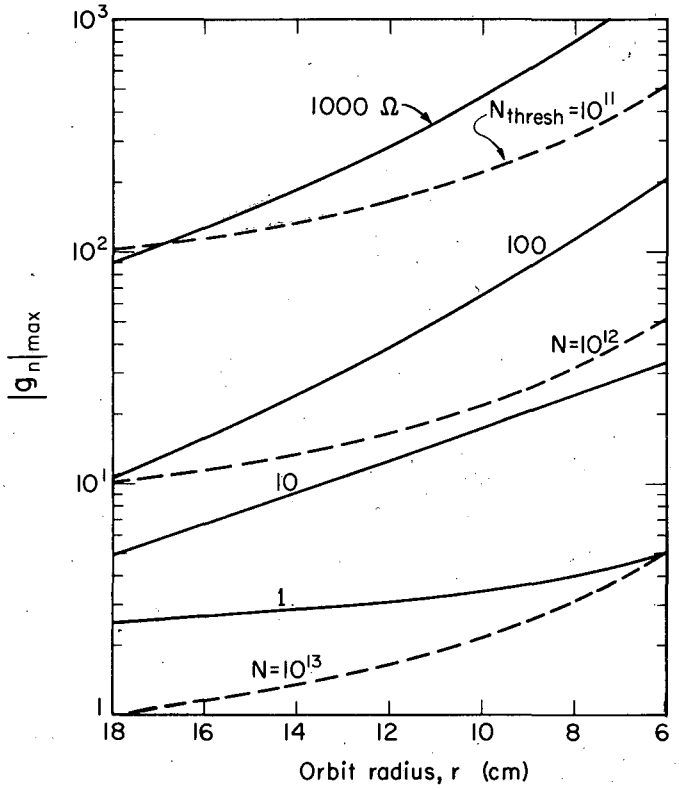

Fig. 4. Ceramic tube. Upper envelope of $|g_n|$ vs r for various R_s, and injection conditions of Fig. 2a. Stability thresholds are for energy spread $\Delta E/E = 2\%$ (c.f. Eq. 9).

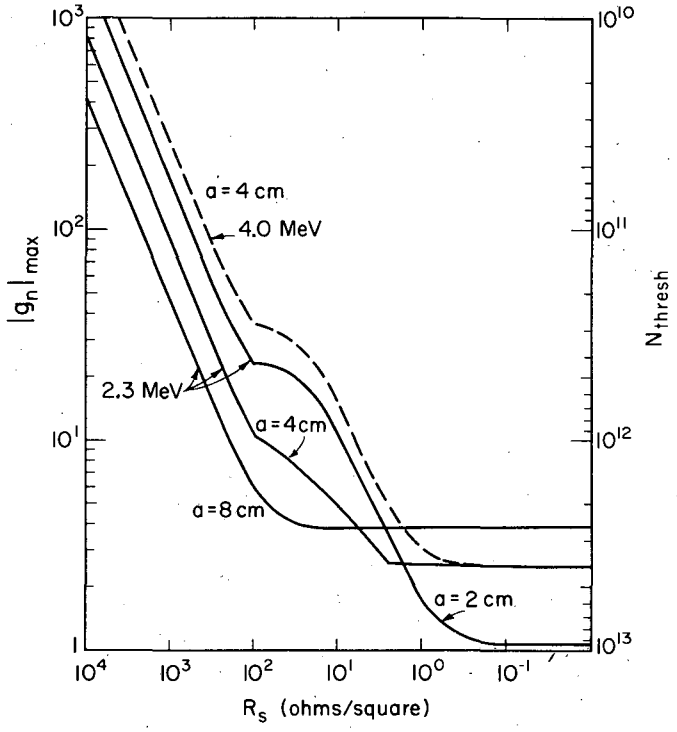

Fig. 5. Ceramic tube. $|g_n|_{max}$ vs R_s at injection for wall inner radius a = 2,4, and 8 cm. Stability threshold scale at right is for 2.3 MeV, and $\Delta E/E = 2\%$.

should be close to the beam. It is important to note that decreasing R_s below 1Ω does not decrease $|g_n|$ significantly.

3. Pillbox Model

Consider now a pillbox of radius A and width H containing an axially centered ring of current of width 2b and zero radial extent at radius r. Assuming, again, a density modulation $\frac{N_n}{2\pi r} e^{i(n\theta-\omega t)}$, the usual eigenmode expansion[4] for the pillbox gives an azimuthal electric field averaged over the axial dimension of the beam:

$$\langle E_n \rangle = -\frac{ieN_n n}{2\pi r^2\gamma^2}\left[-\sum_{\alpha^{TE},p}\frac{16Hr^3\gamma^2}{n\pi b^2}\frac{(\frac{\omega}{c})(\frac{\omega_0}{c})\alpha^2}{(\alpha^2A^2-n^2)}\right.$$

$$\times\ \frac{J_n'^2(\alpha r)}{J_n^2(\alpha A)}\ \frac{\sin^2((2p+1)\pi b/H)}{(2p+1)^2\left[\frac{\omega_E^2}{c^2}-\frac{\omega^2}{c^2}-\frac{i\omega_E\omega}{Q_Ec^2}\right]}$$

$$-\sum_{\alpha^{TM},p}\frac{16\pi nr\gamma^2}{Hb^2}\ \frac{(\frac{\omega}{c})(\frac{\omega_0}{c})}{\alpha^2A^2}\ \frac{J_n^2(\alpha r)}{J_{n+1}^2(\alpha A)}$$

$$\times\ \frac{\sin^2((2p+1)\pi b/H)}{\left(\frac{\omega_E^2}{c^2}\right)\left[\frac{\omega_E^2}{c^2}-\frac{\omega^2}{c^2}-\frac{i\omega_E\omega}{Q_Ec^2}\right]}$$

$$\left.+\sum_{\alpha^{IC},p}\frac{16Hr\gamma^2}{\pi A^2b^2}\ \frac{J_n^2(\alpha r)}{J_{n+1}^2(\alpha A)}\ \frac{\sin^2((2p+1)\pi b/H)}{(2p+1)^2\ \frac{\omega_E^2}{c^2}}\right] \quad (4)$$

where $\alpha^{TE,TM,IC}$ are determined by

$$J_n'(\alpha^{TE}A) = J_n(\alpha^{TM}A) = J_n(\alpha^{IC}A) = 0, \quad \text{respectively,}$$

which follow from the boundary conditions for conducting walls. The superscripts refer to TE, TM and Instantaneous Coulomb fields. The angular velocity of the beam is ω_o and ω_E denotes the pillbox eigenfrequencies:

$$\omega_E^{TE,TM,IC} = c[(\alpha_{mn}^{TE,TM,IC})^2 + (2p+1)^2\,\pi^2/H^2]^{\frac{1}{2}}, \quad (5)$$

where m and n refer to the m^{th} zero of the Bessel function of order n, or its derivative, and (2p + 1) refers to the order of the axial eigenfunction. The losses in the system are accounted for by assigning to each eigenmode a quality factor Q_E.

The quantity in the square brackets in Eq. (1) is g_n. Resonances occur when $\omega \sim \omega_E \sim n\omega_o$, which is possible only for beam radii such that $r \leqslant A\beta$. The radii at which resonances occur increase with n and decrease with m and p and the radii of the TE resonances are greater than the radii of the TM modes. For Q_E large enough that the width of a resonance

is small compared to the spacing, a single term will dominate the sum for g_n near a resonant radius. In that case

$$g_n \approx g^{TE,TM}(n,m,p) \quad \frac{y}{(1 - y^2 - iy/Q_E)} \qquad (6)$$

where $y = \omega/\omega_E$. The coefficients $g^{TE,TM}(n,m,p)$ are always negative, are proportional to γ^2 and for $\beta \approx 1$ have the dependence upon n,m,p shown in Table I.

Table I.

n	m	p	g^{TE}	g^{TM}
$n\to\infty$	1	0	n^{-2}	$n^{-10/3}$
n	$m\to\infty$	p	m^{-1}	m^{-2}
n	m	$p\to\infty$	p^{1-2n}	p^{1-2n}

Values of g_n were obtained by analytically summing Eq. (2) over the index p with $Q = \infty$ away from resonance. The sum over the Bessel functions was done by computer and included the first few hundred terms. The contribution from the remaining terms is typically less than one percent of the total sum. The results for a pillbox of radius 23 cm and height 10 cm are presented in Fig. 6 for mode numbers 1,5,8 as a function of orbit radius as the ring is compressed from injection at 18 cm with half width 1 cm. The injection energy is 2.3 MeV. As in the pipe model the compression cycle is simulated by scaling the beam momentum and width as 1/r and r respectively. For n = 5,8, $|g_n|$ is plotted only to where the first two resonances occur. At these points g_n was calculated from Eq. (6) with y = 1 and Q = 100. Figure 7 is a plot of g_n for the TE and TM resonances with m = 1, p = 0 that the beam encounters during compression, taking Q = 10. These resonances are approximately the strongest the beam encounters (see Table I). Mode numbers of the resonances are labeled on the graph. Values of g_n which lie below the curve labeled $\Delta E/E = 2\%$, $N = 10^{12}$ are stable for 10^{12} electrons with a 2% energy spread.

4. Growth Rates and Stability

For zero energy spread in the beam the dispersion relation[5] requires that the frequency of the density modulation ω satisfy the equation

$$1 = \frac{Nr_e}{2\pi r} \frac{\eta}{\gamma^3} \frac{n^2\omega_o^2}{(n\omega_o - \omega)^2} g_n(\omega) \qquad (7)$$

where r_e is the classical electron radius, $\eta = (p/\omega_o)(d\omega_o/dp) = \gamma^{-2} - \nu_r^{-2}$, and N is the number of electrons. If $g_n(\omega)$ is independent of frequency this equation gives an expression for the e-folding time τ_e:

$$\tau_e^{-1} = n\omega_o \left| \frac{Nr_e}{2\pi r} \frac{\eta}{\gamma^3} g_n \right|^{\frac{1}{2}} \qquad (8)$$

At injection (2.3 MeV, 18 cm) with 10^{12} electrons, e-folding times of approximately 40 and 10 nanoseconds are calculated for mode numbers 1 and 5 in the pillbox (Fig. 6).

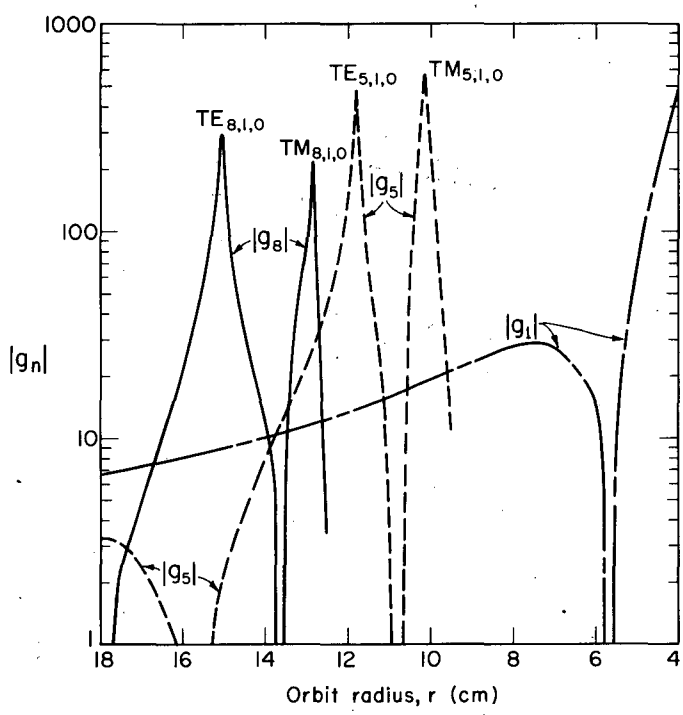

Fig. 6. Pillbox model. $|g_n|$ vs r of a ring during compression with injection radius = 18 cm, axial half-width = 1 cm, energy 2.3 MeV, for modes n = 1,5,8 and with A = 23 cm, H = 10 cm.

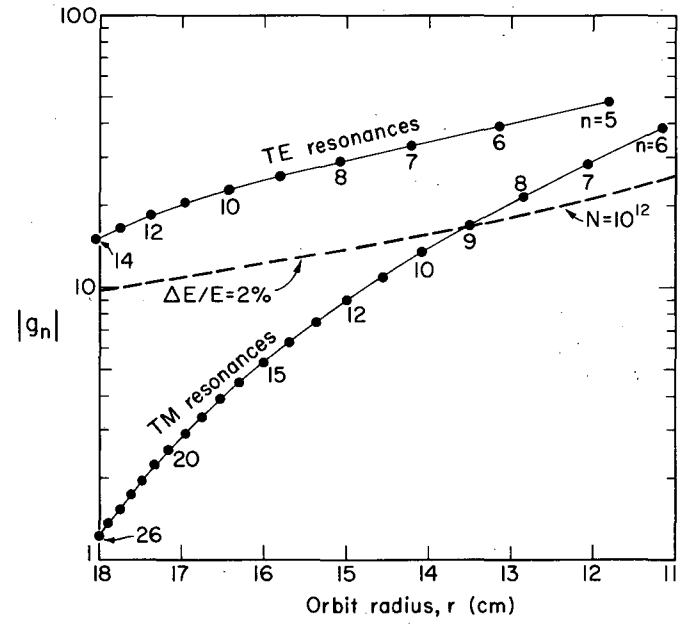

Fig. 7. Pillbox model. Values of $|g_n|$ at resonant peaks traversed by beam during compression, for Q = 10, and stability threshold for $N = 10^{12}$, $\Delta E/E = 2\%$.

For the ceramic pipe, growth rates decrease with decreasing surface resistance R_s. The seventh mode grows with an e-folding time of 20 ns for $R_s = 1000\Omega$, while for $R_s = 50\Omega$ the first mode dominates stability and has an e-folding time ≈ 40 ns.

To calculate resonance growth rates in the pillbox, $g_n(\omega)$ has been given the frequency dependence shown in Eq. (6). For the first TE resonance (n = 14, m = 1,

$p = 0$; Fig. 7) and Q values from 10 to 10,000, we find $\tau_e \approx 2$nsec and real frequency shifts $1 - \omega/n\omega_o \approx 0.01$. It is interesting that these growth rates are comparable with what would be predicted from Eq. (8) with a constant g_n calculated at the peak of the resonance with a $Q = 10$ as in Fig. 7.

Although the growth times in the absence of Landau damping do vary with the resistance of the coating and other parameters, they are always unacceptably short. Therefore it is necessary to have sufficient energy spread and small enough g-values to give stability.

Ruggiero and Vaccaro[6] have obtained solutions of the dispersion relation for the case that the fields are not strongly frequency dependent. The calculations described above for the coated ceramic tube show that this is the case if the surface resistance $R_s < 100\Omega$. We believe that the compressor is probably a sufficiently leaky "pillbox" to limit the pillbox mode resonant Q-values to ten or so. Therefore, to interpret the computed g-values in terms of stability, we shall apply the results of Ref. 6, which for a wide range of energy distributions, lead to the conservative stability condition

$$\frac{r_e}{r} \frac{\beta^2}{\eta\gamma^3} \frac{N|g_n|}{(\Delta E/E)^2} \lesssim 1 \qquad (9)$$

where $\Delta E/E$ is the relative full width at half maximum energy spread.

Threshold values of $|g_n|$ calculated from Eq. (4) for a few intensities N and energy spreads $\Delta E/E$ are shown in Figs. 4, 5, and 7. For the ceramic pipe, it can be seen from Fig. 4 that wall coatings with $R_s \lesssim 100\Omega$ are required to compress rings with $N > 10^{12}$ if $\Delta E/E = 2\%$. From Fig. 8 it may be deduced that comparable intensities can be obtained if the Q-values of the pillbox resonances are $\lesssim 10$.

5. Conclusion

The two models are contradictory in the sense that the ceramic pipe approach calls for a low-resistance wall to protect the beam from large fields generated by the dielectric, whereas the pillbox model calls for low Q to suppress the eigenmodes associated with a cylindrical cavity. A computer program is being written to provide a better simulation of the compressor than can be obtained from our semi-analytic treatment. However, the results of this paper have proven to be a useful indication of the basic problem by predicting the very rapid growth rates observed above threshold and suggesting that thresholds can be raised substantially by the use of suitable metallic coatings.

In the range of most successful operation, the models lead to similar results, which can be stated as follows: the ceramic must be coated to less than 10 ohms/square and the modes of the cylindrical structure must have effective Q-values of less than 10 in order to achieve intensities of 10^{12} electrons with reasonable energy spread. Further theoretical progress awaits the more sophisticated computational tool.

References

1. See paper G-16, Recent Experiments on Forming Electron-Rings, D. Keefe et al.
2. Longitudinal Instability of Relativistic Particle Beams in Laminated Vacuum Chambers, by B. Zotter, CERN Report ISR-TH/69-35.
3. Longitudinal Instabilities in Intense Relativistic Particle Beams, by C. E. Nielsen, A. M. Sessler, K. R. Symon, Proceedings of the CERN Symposium on High Energy Accelerators, 1959.
4. E. U. Condon, J. Appl. Phys. 12, 129 (1941).
5. V. K. Neil and A. M. Sessler, Rev. Sci. Instr. 36, 429 (1965).
6. Solution of the Dispersion Relation for Longitudinal Stability at an Intense Coasting Beam in a Circular Accelerator, by A. G. Ruggiero and V. G. Vaccaro, CERN report ISR-TH/68-33.

TECHNICAL INFORMATION DIVISION
LAWRENCE RADIATION LABORATORY
UNIVERSITY OF CALIFORNIA
BERKELEY, CALIFORNIA 94720